Compact and Sharp-rejection Dual-band Bandstop Filter Based on Transversal Signal-interaction Concept

Lei-Lei Qiu and Qing-Xin Chu
School of Electronic and Information Engineering
South China University of Technology, Guangzhou 510640, China

Abstract— A compact dual-band bandstop filter with sharp-rejection using transversal signal-interaction, consisting of a transmission line path and a cascaded coupled line path, is proposed. Folded structure is used to decrease the size. By tuning the coupling coefficient and length, the centre frequency and bandwidth can be controlled, respectively. Meanwhile the transmission line impedance and odd-mode impedance can be used to improve the return loss and to allocate the transmission poles to sharp the attenuation rate, independently. A compact dual-band bandstop filter centring at 2.4 GHz and 3.7 GHz prototype is designed and fabricated to verify the validity. The simulation and measurement results agree well.

1. INTRODUCTION

Compact dual-band bandstop filters (DBBSFs) are highly desired in wireless communication system applications for their effective double-sideband spectrum suppression, low passband insertion loss and group delay. Many different methods and structures have been proposed to design DBBSFs [1–7]. In [1], the two-step frequency-variable transformation to the low pass prototype was applied to performe a dual-stopband response. While in [2], composite shunt resonators were implemented. In [3], modified optimum banstop filter with source-load coupled line was introduced to achieve wide dual stopband. For the purpose of miniaturizing and controlling the frequency ratio, SIRs [4, 5], short-[6] and open-circuited [6, 7] stub-loaded resonators were presented. Whereas, due to the single transmission zero in the stopband [1–6], the selectivity of the filters needed to be improved. Thus signal-interference technique [8] with more transmission zeros was used to design sharp-rejection DBBSF.

This letter proposes a novel and compact DBBSF with sharp-rejection using transversal signal-interaction concept, which can be implemented by inlaying two short-circuited resonators out of the two folding coupled stubs. The centre frequency and bandwidth can be controlled mainly by tuning the coupling coefficient and length, respectively. In addition, the return loss and selectivity out of the stopband can be improved by adjust the impedance of the transmission line path and coupled path. Detailed theoretical design, simulation, and experiment results for the proposed DBBSF are demonstrated and discussed.

2. FILTER ANALYSIS AND DESIGN

Figure 1 shows the configuration and ideal circuit of the proposed bandstop filter, which is composed of two main paths. Path 1 is a length of transmission line with the impedance Z_1, while path 2 consists of cascaded short-/open-circuited coupled lines with different electrical length θ_2 and θ_3. All coupled lines have the same odd-/even-mode impedance (Z_{oo} and Z_{oe}). All I/O lines are with the impedance of 50 Ω.

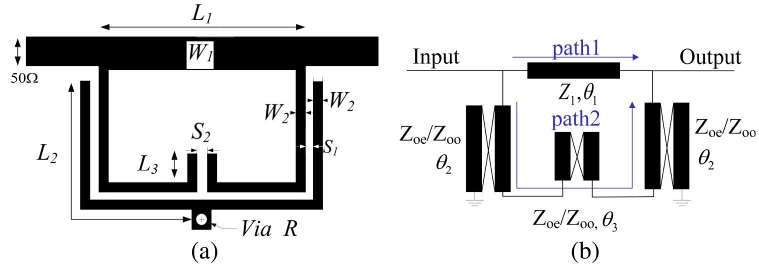

Figure 1: (a) The configuration and (b) ideal circuit of the proposed DBBSF.

According to [9], the $ABCD$ matrices of the shorted/open coupled lines (M_{s1}/M_{s2} and M_o) and two paths are

$$M_{s1} = \begin{bmatrix} A & B \\ C & D \end{bmatrix}, \quad M_{s2} = \begin{bmatrix} D & B \\ C & A \end{bmatrix} \tag{1}$$

$$A = \frac{2Z_{oe}Z_{oo}(1+\cos^2\theta_2) - \sin^2\theta_2(Z_{oe}+Z_{oo})}{4Z_{oe}Z_{oo}\cos\theta_2}, \quad D = \cos\theta_2 \tag{2}$$

$$B = j\frac{(Z_{oe}+Z_{oo})\sin\theta_2}{2}, \quad C = j\frac{(Z_{oe}+Z_{oo})\sin\theta_2}{2Z_{oe}Z_{oo}} \tag{3}$$

$$M_o = \frac{1}{Z_{oe}-Z_{oo}} \begin{bmatrix} Z_{oe}+Z_{oo} & -j2Z_{oe}Z_{oo}\cot\theta_3 \\ j2\tan\theta_3 & Z_{oe}+Z_{oo} \end{bmatrix} \tag{4}$$

$$\begin{bmatrix} A_1 & B_1 \\ C_1 & D_1 \end{bmatrix}_{\text{path1}} = \begin{bmatrix} \cos\theta_1 & jZ_1\sin\theta_1 \\ j\sin\theta_1/Z_1 & \cos\theta_1 \end{bmatrix}, \begin{bmatrix} A_2 & B_2 \\ C_2 & D_2 \end{bmatrix}_{\text{path2}} = M_{s1}\times M_o \times M_{s2} \tag{5}$$

After $ABCD$- and Y-parameter conversions, the S-parameters of the $DBBSF$ can be express as

$$S_{11} = \frac{Y_0^2 - Y_{11}^2 + Y_{21}^2}{(Y_0+Y_{11})^2 - Y_{21}^2}, \quad S_{21} = j\frac{-2Y_{21}Y_0}{(Y_0+Y_{11})^2 - Y_{21}^2} \tag{6}$$

where $Y_0 = 1/Z_0(Z_0 = 50\,\Omega)$, $Y_{11} = D_1/B_1 + D_2/B_2$, $Y_{21} = -1/B_1 - 1/B_2$.

Transmission zeros can be obtained when $S_{21} = 0$. Fig. 3 plots the calculated transmission zeros (f_{tz1}, f_{tz2}, f_{tz3} and f_{tz4}) against K and θ_3 according to (6). When keep Z_{oo} and Z_1 constant, f_{tz1} and f_{tz2} decrease while f_{tz3} and f_{tz4} increase as the increasing of K. Therefore, the frequency ratio f_2/f_1 of the two stopbands can be controlled and larger K will obtain larger f_2/f_1. When θ_3 is zero, the selectivity is poor as only one visible transmission zero is in each stopband. With the increasing of S, f_{tz1} and f_{tz2} (f_{tz3} and f_{tz4}) separate each other with a larger bandwidth.

To explain the characteristics of the filter, Variation of simulated filter characteristic with Z_{oo} and Z_1 are simulated by Agilent Advanced Design System (ADS) and plotted. As can be seen from Figs. 3(a) and (b), the changes of Z_{oo} and Z_1 have no significant effect on transmission zeros while have influence on the characteristic out of the band. The increase of Z_{oo} or decrease of Z_1 will result in the moving of transmission poles to transmission zeros thus sharps the selectivity. Moreover, it should be noted that the impedance Z_1 of the transmission line may be used to improve the return loss out of stopband.

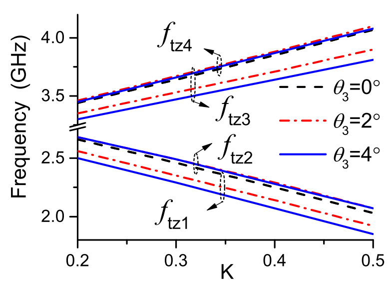

Figure 2: Variation of calculated transmission zeros with K and θ_3 ($Z_{oo} = 90\,\Omega$, $Z_1 = 60\,\Omega$).

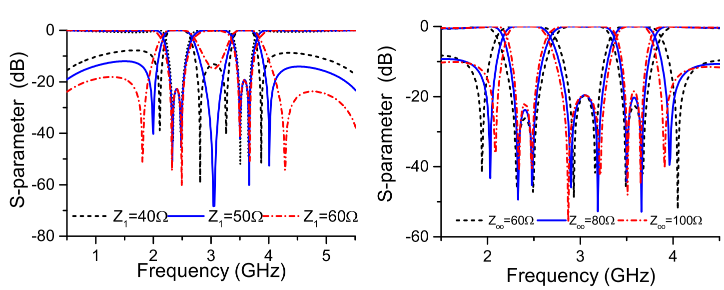

Figure 3: Variation of simulated filter characteristic with Z_{oo}, Z_1 ($K = 0.3$, $\theta_3 = 3$).

From above we know that since the introduction of proposed structure, the centre frequencies and bandwidths in the stopbands can be independently controlled through coupling strength K and electrical length θ_3. In addition, the impedance of the transmission line and odd-impedance of the coupled line can be independently used to adjust the return loss and selectivity out of the stopband. All this make the design of the proposed filter more flexibility.

To clarify the proposed filter design, a proposed DBBSF centring at 2.4 GHz and 3.7 GHz with a relative fractional bandwidth BW_Z of 6% and 4.6%, is designed and implemented. Considering that $f_2/f_1 = 1.5417$ and the requirement of bandwidth, $f_{tz1} = 2.33$ GHz, $f_{tz2} = 2.47$ GHz, $f_{tz3} = 3.65$ GHz and $f_{tz4} = 3.8$ GHz. Through (6), we can obtain that $K = 0.33$ and $\theta_3 = 3$. Z_{oo} and Z_1 are 88 Ω and 45.5 Ω to achieve the isolation up to 20 dB. The configuration of the filter are demonstrated in Fig. 1(a) and the simulated results are shown in Fig. 4. Four transmission zeros are located at 2.33 GHz, 2.461 GHz, 3.67 GHz and 3.79 GHz. The two stopband have a relative 20 dB fabrication bandwidth (FBW) of 8.7% and 5.2%, respectively. The insertion loss is less than 0.35 dB, while the return loss is over 20 dB between the stopbands.

3. RESULTS

The proposed filter is fabricated on the substrate with a relative dielectric constant of 2.55, thickness of 0.8 mm and loss tangle of 0.0029. Fig. 4 illustrates the photograph and measurement result of the DBBSF, the filter has a compact size of only $0.22\lambda_g \times 0.15\lambda_g$ (λ_g is the free space wavelength at the centre frequency of the first stopband). The filter is measured by Agilent 5230 vector network analyzer.

It is shown that more than 25 dB rejection can be achieved in 2.41 GHz and 3.75 GHz with a relative 20 dB FBW of 8.8% and 5%, respectively. The return loss between the two stopbands is about 20 dB. The insertion loss is less than 0.7 dB up to 2.03 GHz while within 1 dB from 4 GHz to 7 GHz. The attenuation rates at the passband to stopband are 174 dB/GHz (measured attenuations being 5.062 dB and 19.96 dB at 2.21 and 2.3 GHz) and 168 dB/GHz (measured attenuations being 19.92 dB and 4.986 dB at 3.85 and 3.94 GHz). The variance between measurement and simulation mainly due to dielectric loss, fabrication tolerance and the loss of SMA connector. To further demonstrate the performances of this filter, the comparisons of measured results for several reported DBBSFs [2–8] are shown in Table 1. The proposed filter shows miniaturization and sharp skirt selectivity.

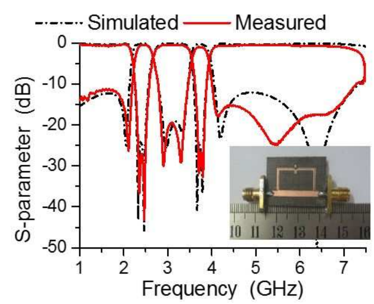

Figure 4: The simulated and measured response of the proposed DBBSF.

Table 1: Comparison with the reported DBBSFs.

Ref.	ILmax (dB)	RL (dB) (dB)	Attenuation Slope (dB/GHz)		TZ	Size ($\lambda_g * \lambda_g$)
			Lower	Upper		
[2]	3	15	139	110	1	0.71*0.59
[3]	3.5	23	79	93	1	0.46*0.21
[4]	3	20	90	112	1	0.29*0.25
[5]	1.5	20	67	72	1	0.24*0.23
[6]	1	20	143	87	1	0.85*0.3
	1	15	80	68	1	0.25*0.19
[7]	1	12	32	26	2	0.26*0.18
[8]	2	15	67	122	2	0.49*0.26
This Work	1	20	174	168	2	0.22*0.15

4. CONCLUSION

In this paper, a compact and sharp-rejection dual-band bandstop filter has been proposed using signal-interaction concept. The filter model has been introduced to analysis the transmission zeros and the effect of parameters on the filter characteristic. Due to four parameters independently control the frequency ratio, bandwidth, return loss and selectivity, the design of the filter is simple and flexible. Finally, the proposed DBBSF is designed, fabricated and measured. Agreement between simulation and measurement verifies the validation of the analyses.

ACKNOWLEDGMENT

This work was supported by the National Natural Science Foundation of China (61171029 and 61101016), the Fundamental Research Funds for the Central Universities (2013ZP0018) and the Guangzhou Science and Information Technology Project (201300000029).

REFERENCES

1. Uchida, H., H. Kamino, et al., "Dual-band-rejection filter for distortion reduction in RF transmitters," *IEEE Trans. Microwave Theory Tech.*, Vol. 52, No. 11, 2550–2556, 2004.
2. Ma, Z., K. Kikuchi, et al., "Novel microstrip dual-band bandstop filter with controllable dual-stopband response," *Proceedings of the AsiaCPacific Microwave Conference*, 1174–1177, 2006.
3. Guntupalli, A. B., V. K. Velidi, and S. Sanyal, "Compact Dual wide bandstop filter," *Proceedings of the Applied Electromagnetics Conference (AEMC)*, 1–4, 2009.
4. Chin, K. S., J. H. Yeh, et al., "Compact dual-band bandstop filters using stepped-impedance resonators," *IEEE Microw. Wireless Compon. Lett.*, Vol. 17, No. 12, 849–851, 2007.
5. Velidi, V. K., A. B. Guntupalli, et al., "Compact tapped stepped impedance open stub dual-band bandstop filters with sharp rejection characteristics," *Microw. Opt. Technol. Lett.*, Vol. 51, No. 10, 2274–2277, 2009.
6. Gao, L., S. W. Cai, et al., "Dual-band bandstop filter using open and short stub-loaded resonators," *Proceedings of the Microwave and Millimeter Wave Technology*, 1–3, 2012.
7. Chen, F. C., J. M. Qiu, and Q. X. Chu, "Dual-band bandstop filter using stub-loaded resonators with sharp rejection characteristic," *Electron. Lett.*, Vol. 49, No. 5, 351–353, 2013.
8. Feng, W. J., W. Q. Che, S. Y. Shi, and Q. Xue, "Compact dual-wideband bandstop filters based on open-coupled lines and transversal signal-interaction concepts," *IET Microw. Antennas Propag.*, Vol. 7, No. 2, 92–97, 2013.
9. Hong, J. S. and M. J. Lancaster, *Microstrip Filters for RF/Microwave Applications*, John Wiley & Sons, New York, 2001.